Characterizing the Heterogeneity of CD8 Inflammation in Biopsied Tumor Tissues Using Novel Image Analysis Techniques

Charles Caldwell[1], Will Paces[1], Austin Greaves[1], Christopher Bruckner[2], Si Tuen Lee-Hoeflich[2], Cris Luengo[1], Roberto Gianani[1]

[1]Flagship Biosciences, [2]Scholar Rock

POSTER #3137

Abstract

One of the most studied immune cells in IO is the cytotoxic CD8 T cell, whose biological function is to identify and destroy infected or dysfunctional cells. The function of the CD8 T cell is complicated by numerous factors within the tumor microenvironment (TME). Tumor cells can aberrantly express immune checkpoint molecules designed to stop CD8 T cells from performing their tumor killing function. Additionally, the function of CD8 T cells may be perturbed by other immune modulating factors within the TME. IO drugs modulating tumor and immune cell interactions such as PD-L1 checkpoint inhibitors have shown that an inflammatory TME, represented by high CD8 presence in the tumors (inflamed tumors), is indicative of a better therapeutic response rate.

Investigation of CD8 T cell status in biopsied tissues typically describes each tissue as one of three main phenotypes: Immune Desert, Immune Excluded, or Inflamed. Immune Desert phenotypes do not express appreciable levels of CD8 throughout the tissue. Immune Excluded tissues contain CD8, but the expression is almost exclusively localized to the stroma surrounding tumor nests. Inflamed tissues show higher percentages of CD8 within the tumor nests of the tissues. While this phenotypic categorization is informative, these percentages of expression are often calculated as a mean of expression through the tissue and does not take into account the heterogeneous nature of tumor biology. This may result in a tumor containing one highly inflamed tumor nest being averaged out with multiple deserted tumor nests and a tissue categorized as excluded or deserted even though inflammation is present.

To better represent the heterogeneity of inflammation within tumor tissues, we present an image analysis-based algorithm which not only separates out the tumor, stroma, and tumor/stroma margin, but identifies each tumor nest within the tissue as its own discrete object. This allows for the enumeration of number and size of all tumor nests within the tissue, and further quantifies the percentage of CD8 expression within and outside of each tumor nest. Each tumor nest is given its own phenotypic classification of inflamed, excluded, or deserted, and the percentage of tumor nests displaying each phenotype. Within this study, we demonstrate heterogeneity of inflammation assessment alongside standard mean phenotypic evaluations of CD8 expression in non-small cell lung cancer, bladder, and melanoma tumor samples. Practical use in clinical studies can help uncover response or resistance associated phenotypes related to tumor heterogeneity.

Materials & Methods

FFPE tissue blocks of Melanoma, Bladder Cancer, and Non-Small Cell Lung Cancer (NSCLC) were sectioned at 4um and IHC-stained for CD8 expression. Whole-tissue image analysis (IA) was performed via Flagship Biosciences' proprietary IA platform. All cells in each tissue section were identified via AI processes that generated hundreds of morphology, spatial, and staining related features per-cell. Machine learning algorithms stratified cells as belonging to the tumoral or stromal space based on their cellular features. Identified tumor cells were subjected to additional algorithms which created tumor nest objects within each tissue that further stratifies cells as belonging to individual tumor nests within each tissue. Tissue-level and per-tumor-nest CD8 expression data was pulled and represented on a whole-cohort basis. All staining and IA outputs were reviewed by a board-certified, MD pathologist.

Conclusions

- Cellular data which simply averages CD8 expression across the entirety of a tissue section does not accurately represent the amount of inflammation-associated heterogeneity present in tumor samples
- Identifying tumor area objects (tumor nests) within biopsied sections allows for the localization of biomarker expression within and outside of individual tumor nests
- Representing biomarker data by tumor nest object, rather than averaging cells across the tissue, allows one to assess the inherent heterogeneity within each individual tissue section
- Collecting tissue-level data on tumor nest inflammation can represent the heterogeneity of inflammation across entire cohorts of tissue
- The described method can identify tumor areas which can be further investigated via protein or spatial genomic interrogations to understand mechanisms behind tumor nest phenotypes and/or resistance to inflammation. Incorporation into clinical trials will provide better insights into drug efficacy and resistance.

Machine Learning Stratification of Cells into Tumor, Stroma, and Tumor/Stroma Interface Compartments

Cell Stratification Using Machine Learning

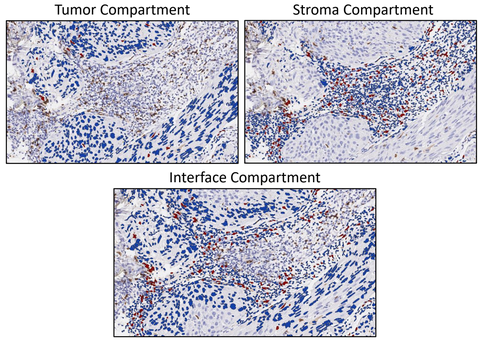

Defining and Scoring Tumor Nest Objects

Parameter	Definition
Minimum Tumor Nest Cells	250 Cells
Minimum Tumor Nest Area	500um
Inflamed Tumor Nest	> 5% CD8+ Cells
Excluded Tumor Nest	< 5% CD8+ cells in tumor nest, > 1% CD8+ cells in peripheral interface
Deserted Tumor Nest	< 5% CD8+ cells in tumor nest, < 1% CD8+ cells in peripheral interface

Visualizing Tumor Nest Objects and Immunophenotypes

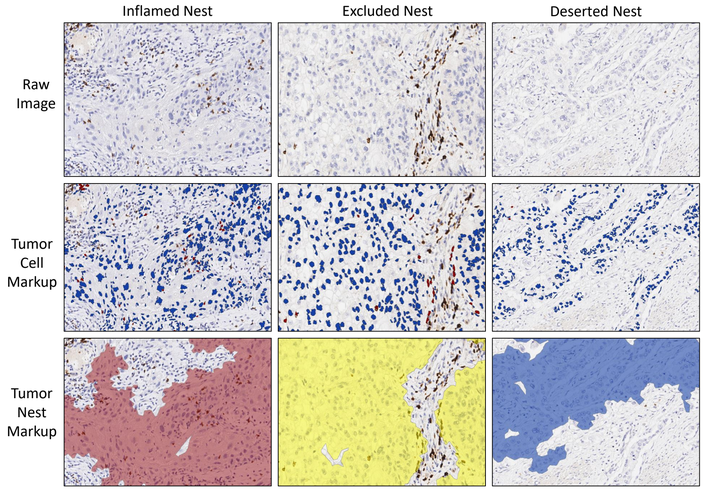

Figure 1| Cell and Tumor Nest Identification Using AI and Machine Learning Techniques. Tissue sections were immunohistochemically stained for CD8 expression using standard processes. Each tissue was analyzed using a proprietary image analysis software which uses AI to find every cell within the tissue and quantify hundreds of morphological and staining-related features. These features were run through machine learning processes in order to separate cells belonging to the tumor compartment from cells within the stromal compartment, then define the interfacial region between the compartments. Digital markup shows CD8 negative (blue) and CD8 positive (red) cells. Additional algorithms were implemented to define each tumor nest as individual objects within the tissues and score each identified tumor nest as immune inflamed (red mask), excluded (yellow mask), or deserted (blue mask) based on the CD8 score within the tumor region and the interfacial region outside each tumor object.

Scoring CD8 Within and Near Individual Tumor Objects

Digital Markup, Tumor Nest Immunophenotypes

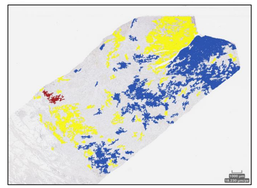

Per-Tissue Tumor Nest Landscape

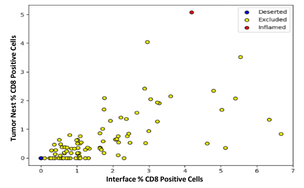

Sample Name	Tumor Nest Number	Tumor Nest Total Cell Count	Tumor Nest CD8 Percent Positive	Interface CD8 Percent Positive	Tumor Nest Status
BladderCA 26	1	281	0	2.308	Excluded
BladderCA 26	2	585	0.513	2.899	Excluded
BladderCA 26	3	703	2.418	2.883	Excluded
BladderCA 26	4	256	5.078	4.181	Inflamed
...	...	...	...	...	...
BladderCA 26	84	405	0	0	Immune Desert
BladderCA 26	85	420	0.238	0.716	Excluded
BladderCA 26	86	250	0	0	Immune Desert
BladderCA 26	87	780	0	0.703	Excluded
BladderCA 26	88	1196	0.0836	0.536	Excluded
BladderCA 26	89	452	0	0.287	Excluded
BladderCA 26	90	445	4.045	2.953	Excluded
BladderCA 26	91	527	0	0.623	Excluded
BladderCA 26	92	1068	0	0.109	Excluded
BladderCA 26	93	910	0.33	0.931	Excluded
BladderCA 26	94	761	0.657	2.111	Excluded
BladderCA 26	95	293	0.341	1.636	Excluded
BladderCA 26	96	336	2.083	5.398	Excluded
BladderCA 26	97	395	0.759	2.143	Excluded
BladderCA 26	98	352	0.284	1.674	Excluded

Figure 2| Representative Tumor Nest Data from Individual Tissues. Per-tissue tumor nest data lists each individual tumor nest identified and associated endpoints. Each tumor nest can be evaluated by the total cellular content, the percentage of CD8 expression in the tumor nest, and the percentage of CD8 expression in the surrounding interfacial region of each tumor nest. Each tissue can be evaluated on its own tumor nest immune landscape presentation. The phenotypic status of each individual tumor nest is additionally derived and represented.

Applying the Developed Method to NSCLC, Melanoma, and Bladder Cancer Cohorts

Representative Images of Tumor Nest Phenotype Markup

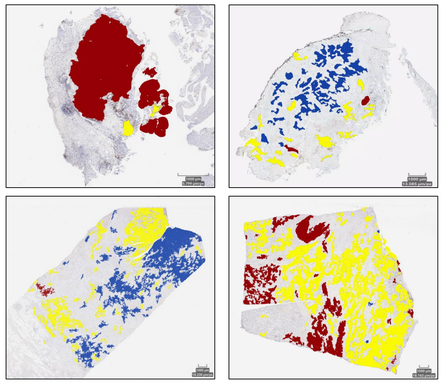

Summary Data, NSCLC Cohort

Unique ID	Tumor Nest Count	Total Tumor Cell Count in Nests	Percent Inflamed Tumor Nests	Percent Excluded Tumor Nests	Percent Desert Tumor Nests
NSCLC_1	18	825399	0	77.8	22.2
NSCLC_2	85	319873	0	89.4	10.6
NSCLC_3	91	545322	0	98.9	1.1
NSCLC_4	116	215276	2.6	97.4	0
NSCLC_5	49	55418	4.1	67.3	28.6
NSCLC_6	21	271083	4.8	95.2	0
NSCLC_7	22	469400	13.6	86.4	0
NSCLC_8	127	157899	17.3	82.7	0
NSCLC_9	5	23005	20	80	0
NSCLC_10	4	480415	25	75	0
NSCLC_11	28	260942	28.6	71.4	0
NSCLC_12	38	379186	31.6	68.4	0
NSCLC_13	139	184264	31.7	68.3	0
NSCLC_14	106	99269	37.7	62.3	0
NSCLC_15	35	69374	40	60	0
NSCLC_16	48	323254	52.1	47.9	0
NSCLC_17	59	319101	52.5	47.5	0
NSCLC_18	14	84406	92.9	7.1	0
NSCLC_19	75	193553	98.7	1.3	0

Evaluating the Tumor CD8 Immunophenotype Landscape of NSCLC, Bladder, and Melanoma Samples

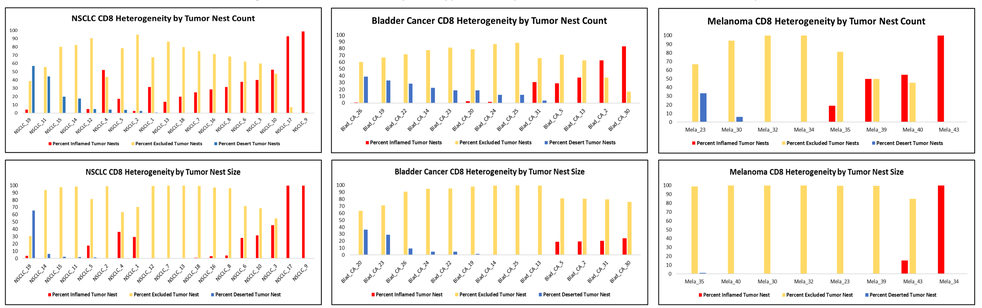

Figure 3| Summary Per-Tumor Nest CD8 Data from NSCLC, Bladder Cancer, and Melanoma Cohorts. Digital markups of tumor nest inflammation (left) are valuable as quick visual assessments of per-tissue tumor nest heterogeneity. Cohort-level summary data (middle table) is provided and can be graphically represented (right) to assess heterogeneity across the entire cohort of tissue. Representation of the percentage of the total number of tumor nests which are inflamed, excluded, or deserted are shown (top right row). The raw number of tumor nests as a percentage may be misleading if, for example, there is a very large inflamed tumor nest and a very small deserted tumor nest. In this case, we show also the normalization of inflammation percentages based on the size of each tumor nest (bottom right row). The total number of tumor nest cells belonging to each tumor nest phenotype were summed and represented as a percentage of the total number of tumor nest cells in each tissue, providing representation of the heterogeneity of inflammation based on the size of each individual tumor nest phenotype. In these cohorts, Melanoma and Bladder tissues were primarily excluded or deserted, while NSCLC tissues had a higher amount of inflamed tumor nests within each tissue.